Composites Communications 45 (2024) 101791



Contents lists available at ScienceDirect

Composites Communications

journal homepage: www.elsevier.com/locate/coco



Short Communication

Hygrothermal effects on translaminar fracture toughness of quasi-isotropic laminates with different stacking sequences

Bowen Gong [a,1], Yuzhong Ge [a,1], Huan Wang [a], Hua-Xin Peng [a,**], Michael R. Wisnom [b], Xiaodong Xu [c,*]

[a] Institute for Composites Science Innovation (InCSI), School of Materials Science and Engineering, Zhejiang University, Hangzhou, 310027, PR China
[b] Bristol Composites Institute, University of Bristol, University Walk, Bristol, BS8 1TR, UK
[c] Centre for Aeronautics, School of Aerospace, Transport and Manufacturing, Cranfield University, Cranfield, MK43 0AL, UK

ARTICLE INFO

Keywords:
Laminates
Fracture toughness
CT analysis
Moisture

ABSTRACT

Hygrothermal effects on the translaminar fracture toughness of the carbon/epoxy composite with two different stacking sequences at 120 °C were studied and the failure mechanisms are explained. The eccentrically loaded single-edge-notch tension (ESET) experiments showed that two different quasi-isotropic stacking sequences ($[90/45/0/-45]_{4s}$ and $[45/90/-45/0]_{4s}$) have negligible difference in translaminar fracture toughness. It was found that the fracture toughness of conditioned specimens at hot temperature wet (HTW) condition increased by 75 % compared to that at room temperature dry (RTD). The average saturated damage height at HTW increased by 48 % compared with that at RTD according to *ex situ* X-ray computed tomography (CT) observation. The larger saturated damage height observed in the 0° plies of the HTW specimens results in the higher translaminar fracture toughness.

1. Introduction

Composite materials are widely used in the aerospace industry, due to the demand for materials with high strength and low density. Some flights experience extreme changes in relative humidity (RH) or relative temperature (e.g. from −54 °C to 71 °C) [1], the performance of composite materials is affected by environmental conditions, for instance high temperature and/or high humidity [2]. The glass transition temperature of aerospace composites is reduced by moisture, thereby decreasing the maximum working temperature [3]. Furthermore, the mechanical properties of the matrix and fibre/matrix interface are affected by temperature [4]. Therefore, research on the mechanical properties of composites in moisture/hot conditions is important for aerospace applications. Liu et al. [5] tested the quasi-static mechanical behavior of epoxy resin in a cyclic hygrothermal aging environment (with humidity changes from 0 to 95 % RH and temperature changes from 70 °C to 100 °C), showing that the elastic modulus and ultimate strength decreased with the duration of the hygrothermal aging cycles, the reason is that the continuous interaction of water molecules and epoxy destroyed the polymer chains.

Translaminar fracture toughness is associated with cracks propagating perpendicular to the fiber direction involving fiber fracture, and has important implications for the damage assessment of notched laminate composites [6–9] and laminates with in-plane [10] and out-of-plane [11] defects. The majority of the previous research of translaminar fracture toughness has been done at room temperature and/or dry conditions [12–15]. Xu et al. [8,16–19] examined the detailed damage within each ply of quasi-isotropic laminates at room temperature and dry condition (RTD). Load drops were observed before the damage zone was fully developed. Xu et al. [19] investigated the size effect of laminates, showing that 0° splitting can blunt the stress concentration at the crack tip, while the double 0° plies have more energy to drive split propagation. Teixeira et al. [14] studied the relationship between the translaminar fracture toughness and the thickness of the 0° layers in cross-ply laminates. It has shown that with the increasing thickness, the length of fiber pull-out increased, which led to much more energy dissipation. However, these works explained damage evolution of translaminar cracks at RTD but not at high temperature and wet

* Corresponding author.
** Corresponding author.
E-mail addresses: hxpengwork@zju.edu.cn (H.-X. Peng), xiaodong.xu@cranfield.ac.uk (X. Xu).
[1] Equal contribution.

https://doi.org/10.1016/j.coco.2023.101791
Received 12 October 2023; Received in revised form 29 November 2023; Accepted 5 December 2023
Available online 9 December 2023
2452-2139/© 2023 The Authors. Published by Elsevier Ltd. This is an open access article under the CC BY license (http://creativecommons.org/licenses/by/4.0/).

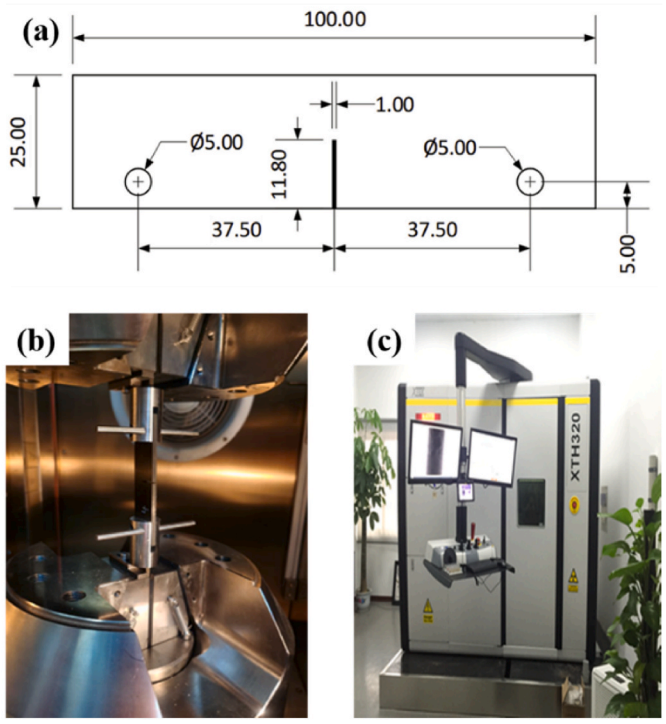


Fig. 1. Specimen and test set-up (**a**) geometry and dimensions of specimen, based on ASTM E1922; (**b**) test jig in chamber; (**c**) CT scanner, NIKON XTH 320 LC CT.

condition (HTW). Marín et al. [20] studied the failure mechanisms of translaminar fracture toughness of cross-ply laminates at three environmental conditions: as received-room temperature, wet-room temperature, wet-high temperature. The highest translaminar fracture toughness was indirectly derived from the scaled double edge-notched tension (DEN-T) specimens conditioned in a wet-high temperature environment (85 % RH and 120 °C), with significant fiber pull out observed on the fracture surface. Yu et al. [21] predicted the effect of hygrothermal including hot-wet conditions (85 % RH and 90 °C) on the translaminar fracture toughness of cross-ply laminates with independently measured properties of the interface. Poor pull-out frictional stress and extensive debonding were believed to lead to improved translaminar fracture toughness at HTW.

This work aims to provide insight into the behavior of quasi-isotropic carbon/epoxy laminates at high temperature and wet conditions. Specifically, this study is to: (1) provide an experimental study of the hygrothermal effects (120 °C testing temperature) on translaminar fracture toughness. (2) analyze the internal crack propagation by using X-ray computed tomography (CT), which explains the failure mechanisms; (3) investigate the effect of stacking sequence on translaminar fracture toughness. To the authors' best knowledge, translaminar fracture toughness of HTW conditioned quasi-isotropic carbon/epoxy laminates has not been reported at 120 °C before, neither have quasi-isotropic laminates with different stacking sequences been compared at HTW.

2. Experimental set-up

The eccentrically loaded single-edge-notch tension (ESET) specimen design and testing process strictly follow the ASTM E1922 standard [22]. The dimensions of the specimen are shown in Fig. 1a. Hexcel's IM7/8552 carbon/epoxy UD prepreg was used. The test panels were divided into two groups featuring different quasi-isotropic stacking sequences, i.e. $[90/45/0/-45]_{4s}$ and $[45/90/-45/0]_{4s}$. The nominal thickness and width of specimens were 4 mm and 25 mm, respectively. The specimens, including the notches, were cut from a plate using 1 mm diameter carbide endmills on a computer numerical controlled (CNC) router. No cutting damage was visible at the holes. The notch tip was extended manually using a precision saw blade with a width of 0.25 mm. After drying in a chamber (70 °C) for 6 hours, these samples were placed in a humidity chamber to be conditioned at 80 °C and 85 % RH for 3 months as per the ASTM D5229/D5229 M standard [23] until two consecutive measurements of mass were within 0.02 % after a week. The final percentage of mass gain was 0.7 %. The specimens were loaded on a 250 kN Zwick/Roell 250SE test machine with loading pins inserted into the two holes in the specimen as per the ASTM E1922 standard [22]. The experimental setup in an environment chamber is shown in Fig. 1b. All tests were carried out at 120 °C in a thermal chamber. A NIKON XTH 320LC X-ray CT scanner was subsequently used to observe the crack propagation of specimens in Fig. 1c. The location, size and morphology of damage were examined with a resolution of 50 μm. The scanning voltage was 100 kV (160 μA) and the exposure time for each radiograph was 500 ms.

3. CT analysis

As shown in Fig. 2, a set of images through the thickness were taken from a CT scan done immediately after a HTW specimen reached the

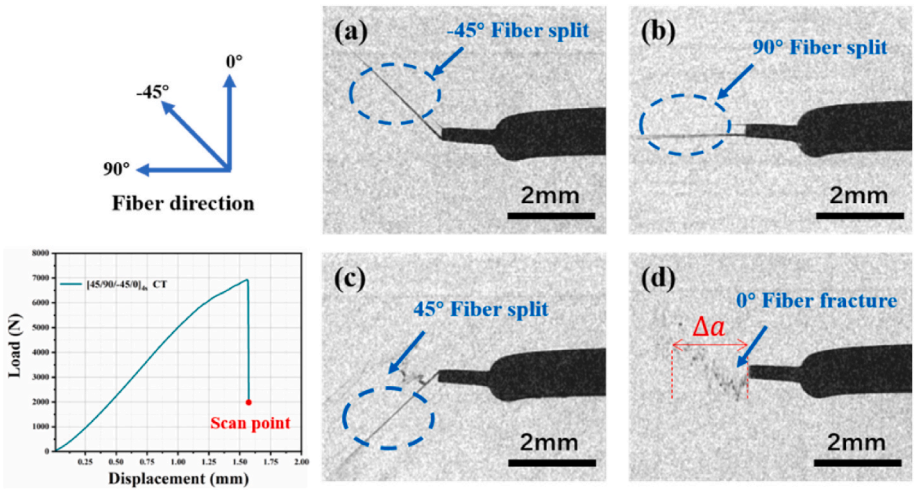


Fig. 2. Typical CT images of damage in (**a**) −45° ply, (**b**) 90° ply, (**c**) 45° ply, (**d**) 0° ply of $[45/90/-45/0]_{4s}$ specimen at HTW. *Note*. These images were captured immediately after the peak load, and Δa is the 0° crack increment.

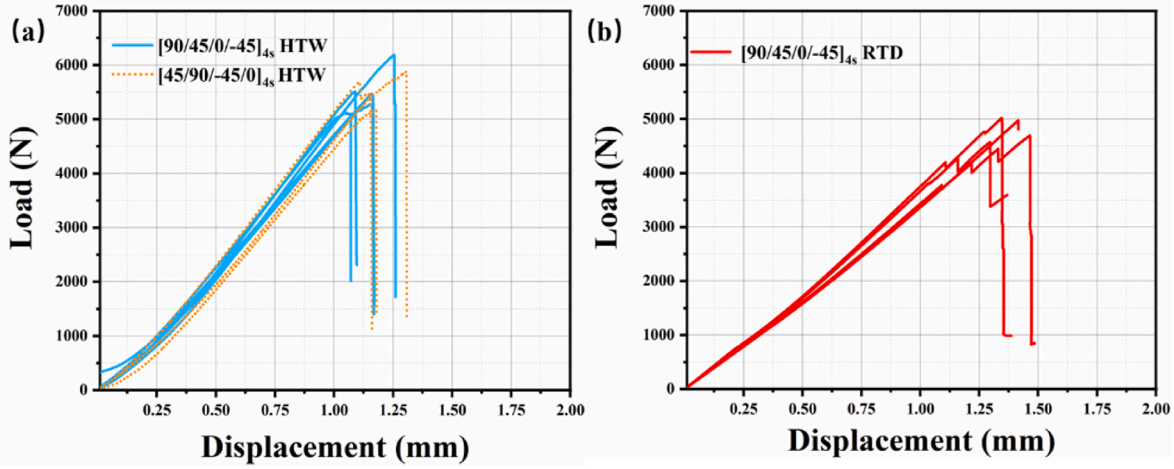


Fig. 3. (**a**) Load-displacement curves of two sets of specimens at HTW. *Note*. The peak load of $[90/45/0/-45]_{4s}$ and $[45/90/-45/0]_{4s}$ are 5514 N ± 407.3 and 5587 N ± 369.3, respectively. (**b**) Load-displacement curves of specimens at RTD. *Note*. The peak load is 4812 N ± 216.3.

peak load. In all of the 90°, −45° and 45° plies, damage such as splitting, and fiber failure could be observed. According to previous *in situ* experimental results of the same specimens at RTD condition [18], 0° ply fracture already occurred before the peak load, and it was found that only after all plies were broken including the ±45° plies, that significant load drops occurred. In the current study at HTW, it was also found that at the peak load all plies are broken including the ±45° plies (Fig. 2c). This indicates that the fracture process zone was fully developed along the direction of translaminar fracture at the large load drop, which is consistent with the previous studies using the same specimen [17,18].

The definition of crack length influences the value of fracture toughness [24]. Here, the effective crack length a was adopted, which consists of two parts: the machined notch length a_N and the size of the fracture process zone Δa. Including the size of the fracture process zone is necessary when Δa is no longer negligible, to make the measured fracture toughness accurate. Here, Δa is quantified by the average fiber breakage length in all 0° plies at HTW, taken as the average value of 1.9 mm from the CT images e.g. in Fig. 2d. This is in comparison to the Δa value of 1.4 mm at RTD [18].

4. Experimental results and data reduction

The load and displacement curves from two sets of HTW tests at Zhejiang University are shown in Fig. 3a, while those tested at RTD using an Shimadzu test machine with a 10 kN load cell at the University of Bristol are also shown in Fig. 3b [18]. The following points were observed: (1) An approximately linear load-displacement relationship is apparent at the beginning of the tests. The initial slopes in Fig. 3a and b are slightly different at different environmental conditions. This is because the displacements were measured at the crossheads of two different machines. However, displacements were not used for data reduction according to the ASTM E1922 standard [22]. A final drop occurred at the peak load (Fig. 3a). No obvious load drops occurred before the peak load at HTW. In contrast, multiple load drops were observed on the load-displacement curves at the RTD as seen in Fig. 3b [18]. The final load drops at both temperatures (room temperature and 120 °C) were accompanied by compression failures at the rear end of the samples. It is believed that the compressive failure occurred after the fracture process zone was fully developed, because the fracture process zone at HTW looks similar to that already fully developed at RTD but larger. The compressive failure stopped any further fracture propagation, but the average maximum load at HTW is already nearly 20 % higher than that at RTD.

The values of translaminar fracture toughness are calculated using Eq. (1) in the ASTM E1922 standard:

$$K_c = \frac{\frac{P}{B\sqrt{W}}\alpha^{\frac{1}{2}}(1.4+\alpha)[3.97-10.88\alpha+26.25\alpha^2-38.9\alpha^3+30.15\alpha^4-9.27\alpha^5]}{(1-\alpha)^{\frac{3}{2}}} \quad (1)$$

where K_C represents the fracture toughness (MPa·m$^{1/2}$), P represents the failure load (MN), a represents the effective crack length (m), B represents the specimen thickness (m), W represents the specimen width (m). $\alpha = a/W$ is based on measured average values and is sensitive to both a and W for the ESET specimen with a small ligament.

The value of fracture energy is calculated using Eq. (2) assuming plane stress:

$$G_c = \frac{K_c^2}{E} \quad (2)$$

where G_c represents the critical energy release rate (kJ/m^2), K_c represents the fracture toughness (MPa·m$^{1/2}$) calculated using Eq. (1). E is the Young's modulus of the quasi-isotropic laminate (GPa), which is 61.6 GPa [25].

In situ and *ex situ* CT scans were conducted previously to measure the crack length and hence translaminar fracture energy of specimens with the same IM7/8552 material and a layup of $[90/45/0/-45]_{4s}$ at RTD [18]. A translaminar fracture energy of 81.1 kJ/m^2 was reported at RTD [18]. In the current experiments, a single translaminar fracture energy value for initial fracture propagation can be determined using the same ESET specimen geometry at HTW with the crack length measured from *ex situ* CT scans. The translaminar fracture energy values of specimens with $[90/45/0/-45]_{4s}$ and $[45/90/-45/0]_{4s}$ stacking sequences are very similar, 142.3 kJ/m^2 and 146.1 kJ/m^2 respectively calculated using Equations (1) and (2). For the specimen with $[90/45/0/-45]_{4s}$ stacking sequence, the translaminar fracture energy at HTW increases by 75 % compared to that at RTD. The same data reduction method as that used in the previous works [17,18] has been adopted in terms of crack length measurements and failure load selections.

5. Discussion

Based on the above experimental results, it was found that the moisture and temperature conditioning lead to increased translaminar fracture toughness of these quasi-isotropic laminates. The potential reasons are summarized as follows:

1) The initial splits in *ex situ* CT scan images of typical 0° plies at RTD and HTW conditions were compared [18]. It was observed that the 0° splitting was longer at HTW than at RTD. The longer 0° fiber

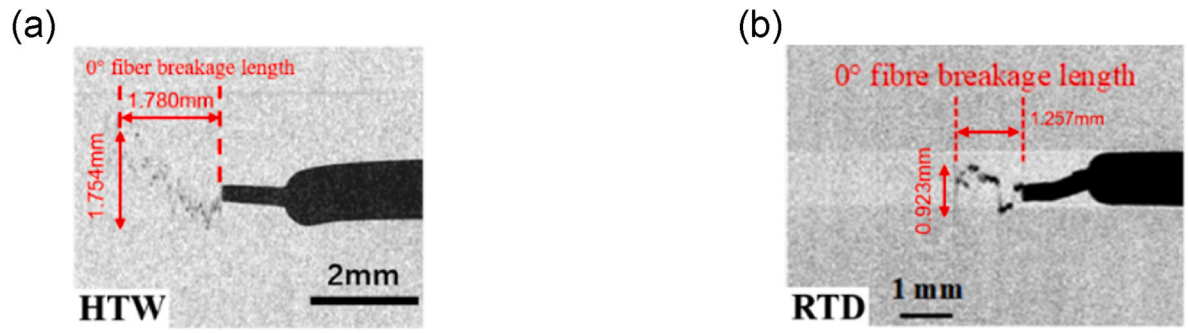


Fig. 4. Typical CT images of 0° plies at (**a**) HTW and (**b**) RTD [18] conditions. *Note*. The saturated damage height at HTW and RTD condition are 1.754 mm and 0.923 mm, respectively.

splitting blunts the stress concentration at the tip of the notch, which retards the fiber breakage [18]. This leads to the increase of failure load at HTW and demonstrates the effect of 0° splits on translaminar fracture toughness.

2) Zobeiry et al. defined the extent of fiber breakage parallel to the 0° fiber direction as the saturated damage height [26]. Compared with the results at RTD, the height of saturated damage at HTW also increases significantly as shown in Fig. 4. The average saturated damage height based on the measurements in the 0° plies is 48 % higher at HTW than that at RTD. This indicates longer fiber debonding or pull-out lengths. As described in Ref. [21], the Mode II fracture toughness decreases with increased temperature and humidity level giving increased fiber pull-out length, thus leading to a larger saturated damage height. A larger saturated damage height in Fig. 4 leads to higher translaminar fracture toughness at HTW.

6. Conclusions

The experimental results presented here demonstrate the influence of temperature and moisture on the translaminar fracture toughness of carbon/epoxy laminates with different quasi-isotropic stacking sequences. During the experiments at hot temperature and wet conditions (HTW), no load drops were observed before the peak load, so a single fracture toughness value for initial fracture propagation can be measured for each layup. It has been shown that the stacking sequence has little effect on the translaminar fracture toughness. It has also been demonstrated that the translaminar fracture energy at HTW is increased by 75 % compared with that at room temperature and dry conditions (RTD). This is owing to the larger saturated damage height at HTW promoting the tougher response. Due to the toughened response at HTW, translaminar fracture propagation is delayed. This study provides new experimental data for quasi-isotropic carbon/epoxy laminates for better understanding the translaminar toughening mechanisms in response to different environmental conditions.

CRediT authorship contribution statement

Bowen Gong: Investigation, Methodology, Project administration, Writing – original draft. **Yuzhong Ge:** Formal analysis, Investigation, Writing – original draft, Data curation. **Huan Wang:** Supervision, Investigation. **Hua-Xin Peng:** Supervision, Writing – review & editing. **Michael R. Wisnom:** Writing – review & editing. **Xiaodong Xu:** Conceptualization, Investigation, Methodology, Resources, Validation, Writing – review & editing.

Declaration of competing interest

The authors declare that they have no known competing financial interests or personal relationships that could have appeared to influence the work reported in this paper.

Data availability

Data will be made available on request.

References

[1] L. Marín, D. Trias, P. Badalló, G. Rus, J. Mayugo, Optimization of composite stiffened panels under mechanical and hygrothermal loads using neural networks and genetic algorithms, Compos. Struct. 94 (11) (2012) 3321–3326.
[2] N. Guermazi, A. Ben Tarjem, I. Ksouri, H.F. Ayedi, On the durability of FRP composites for aircraft structures in hygrothermal conditioning, Compos. B Eng. 85 (2016) 294–304.
[3] F. Jones, J. Foreman, The response of aerospace composites to temperature and humidity, in: Polymer Composites in the Aerospace Industry, Elsevier, 2015, pp. 335–369.
[4] E. Greenhalgh, Failure Analysis and Fractography of Polymer Composites, Elsevier, 2009.
[5] L.L. Liu, K.L. Xu, Y.B. Xu, Z.H. Zhao, G. Luo, W. Chen, Experimental study of quasi-static and dynamic tensile behavior of epoxy resin under cyclic hygrothermal aging, Polym. Degrad. Stabil. 200 (2022).
[6] Y. Geboes, A. Katalagarianakis, J. Soete, J. Ivens, Y. Swolfs, The translaminar fracture toughness of high-performance polymer fibre composites and their carbon fibre hybrids, Compos. Sci. Technol. 221 (2022).
[7] A.R. Torabi, E. Pirhadi, Translaminar notch fracture toughness expressions for composite laminates, Theor. Appl. Fract. Mech. 119 (2022).
[8] X. Xu, X. Sun, M.R. Wisnom, Initial R-curves for trans-laminar fracture of quasi-isotropic carbon/epoxy laminates from specimens with increasing size, Compos. Sci. Technol. 216 (2021), 109077.
[9] M. Laffan, S. Pinho, P. Robinson, A. McMillan, Translaminar fracture toughness testing of composites: a review, Polym. Test. 31 (3) (2012) 481–489.
[10] B. Gong, W. Ouyang, M. Nartey, H. Wang, K.D. Potter, H.-X. Peng, Minimizing the in-plane damage of Z-pinned composite laminates via a pre-hole pin insertion process, Compos. Sci. Technol. 200 (2020), 108413.
[11] M. Nartey, T. Zhang, B. Gong, J. Wang, S. Peng, H. Wang, H.-X. Peng, Understanding the impact of fibre wrinkle architectures on composite laminates through tailored gaps and overlaps, Compos. B Eng. 196 (2020), 108097.
[12] S.T. Pinho, P. Robinson, L. Iannucci, Fracture toughness of the tensile and compressive fibre failure modes in laminated composites, Compos. Sci. Technol. 66 (13) (2006) 2069–2079.
[13] M. Laffan, S. Pinho, P. Robinson, L. Iannucci, Measurement of the in situ ply fracture toughness associated with mode I fibre tensile failure in FRP. Part I: data reduction, Compos. Sci. Technol. 70 (4) (2010) 606–613.
[14] R.F. Teixeira, S.T. Pinho, P. Robinson, Thickness-dependence of the translaminar fracture toughness: experimental study using thin-ply composites, Compos. Appl. Sci. Manuf. 90 (2016) 33–44.
[15] V. Médeau, F. Laurin, J. Rannou, A. Hurmane, H. Quillent, F. Lachaud, Robust characterization of crack propagation in 3D woven composites and evidences of size dependency, Compos. Struct. 225 (2019), 111175.
[16] X. Xu, M.R. Wisnom, Y. Mahadik, S.R. Hallett, Scaling of fracture response in Over-height Compact Tension tests, Compos. Appl. Sci. Manuf. 69 (2015) 40–48.
[17] X. Sun, S. Takeda, M.R. Wisnom, X. Xu, In situ characterization of trans-laminar fracture toughness using X-ray Computed Tomography, Compos. Commun. 21 (2020), 100408.
[18] X. Xu, S. Takeda, M.R. Wisnom, Investigation of fracture process zone development in quasi-isotropic carbon/epoxy laminates using in situ and ex situ X-ray Computed Tomography, Compos. Appl. Sci. Manuf. 166 (2023), 107395.
[19] X. Xu, M.R. Wisnom, Y. Mahadik, S.R. Hallett, An experimental investigation into size effects in quasi-isotropic carbon/epoxy laminates with sharp and blunt notches, Compos. Sci. Technol. 100 (2014) 220–227.
[20] L. Marin, E.V. Gonzalez, P. Maimi, D. Trias, P.P. Camanho, Hygrothermal effects on the translaminar fracture toughness of cross-ply carbon/epoxy laminates: failure mechanisms, Compos. Sci. Technol. 122 (2016) 130–139.
[21] B. Yu, T.J. Katafiasz, S. Nguyen, G. Allegri, J. Finlayson, E.S. Greenhalgh, S. T. Pinho, S. Pimenta, Hygrothermal effects on the translaminar fracture toughness

of a highly toughened aerospace CFRP: experimental characterisation and model prediction, Compos. Appl. Sci. Manuf. 150 (2021).
[22] ASTM E1922-97, Standard Test Method for Translaminar Fracture Toughness of Laminated Polymer Matrix Composite Materials, ASTM International, West Conshohocken, PA, USA, 1997.
[23] ASTM D5229/D5229M-2014, Standard test method for moisture absorption properties, And Equilibrium Conditioning of Polymer Matrix Composite Materials, ASTM International, USA, 2014.
[24] X. Xu, M.R. Wisnom, S.R. Hallett, Deducing the R-curve for trans-laminar fracture from a virtual Over-height Compact Tension (OCT) test, Compos. Appl. Sci. Manuf. 118 (2019) 162–170.
[25] X. Xu, M.R. Wisnom, X. Li, S.R. Hallett, A numerical investigation into size effects in centre-notched quasi-isotropic carbon/epoxy laminates, Compos. Sci. Technol. 111 (2015) 32–39.
[26] N. Zobeiry, R. Vaziri, A. Poursartip, Characterization of strain-softening behavior and failure mechanisms of composites under tension and compression, Compos. Appl. Sci. Manuf. 68 (2015) 29–41.



https://dspace.org/

Hygrothermal effects on translaminar fracture toughness of quasi-isotropic laminates with different stacking sequences

Gong, Bowen; Ge, Yuzhong; Wang, Huan; Peng, Hua-Xin; Wisnom, Michael R. ...

2024-01-01
Elsevier
https://doi.org/10.1016/j.coco.2023.101791
Gong B, Ge Y, Wang H, et al., (2024) Hygrothermal effects on translaminar fracture toughness of quasi-isotropic laminates with different stacking sequences. Composites Communications, Volume 45, January 2024, Article number 101791

Downloaded from a DSpace repository. https://dspace.org/